Open Access

Sperm Biology

ORIGINAL ARTICLE

The role of tyrosine phosphatase Shp2 in spermatogonial differentiation and spermatocyte meiosis

Yang Li[1,*], Wen-Sheng Liu[1,*], Jia Yi[1], Shuang-Bo Kong[2], Jian-Cheng Ding[1], Yi-Nan Zhao[1], Ying-Pu Tian[1], Gen-Sheng Feng[4], Chao-Jun Li[5], Wen Liu[1,3], Hai-Bin Wang[2], Zhong-Xian Lu[1,2,3]

The transition from spermatogonia to spermatocytes and the initiation of meiosis are key steps in spermatogenesis and are precisely regulated by a plethora of proteins. However, the underlying molecular mechanism remains largely unknown. Here, we report that Src homology domain tyrosine phosphatase 2 (Shp2; encoded by the protein tyrosine phosphatase, nonreceptor type 11 [*Ptpn11*] gene) is abundant in spermatogonia but markedly decreases in meiotic spermatocytes. Conditional knockout of *Shp2* in spermatogonia in mice using stimulated by retinoic acid gene 8 (*Stra8*)-*cre* enhanced spermatogonial differentiation and disturbed the meiotic process. Depletion of *Shp2* in spermatogonia caused many meiotic spermatocytes to die; moreover, the surviving spermatocytes reached the leptotene stage early at postnatal day 9 (PN9) and the pachytene stage at PN11–13. In preleptotene spermatocytes, *Shp2* deletion disrupted the expression of meiotic genes, such as disrupted meiotic cDNA 1 (*Dmc1*), DNA repair recombinase rad51 (*Rad51*), and structural maintenance of chromosome 3 (*Smc3*), and these deficiencies interrupted spermatocyte meiosis. In GC-1 cells cultured *in vitro*, *Shp2* knockdown suppressed the retinoic acid (RA)-induced phosphorylation of extracellular-regulated protein kinase (Erk) and protein kinase B (Akt/PKB) and the expression of target genes such as synaptonemal complex protein 3 (*Sycp3*) and *Dmc1*. Together, these data suggest that Shp2 plays a crucial role in spermatogenesis by governing the transition from spermatogonia to spermatocytes and by mediating meiotic progression through regulating gene transcription, thus providing a potential treatment target for male infertility.
Asian Journal of Andrology (2020) 22, 79–87; doi: 10.4103/aja.aja_49_19; published online: 14 June 2019

Keywords: cell differentiation; gene expression; spermatogenesis; transgenic mouse

INTRODUCTION

Spermatogenesis is a consecutive cellular differentiation process. In the fetal mouse testis, gonocytes undergo self-renewal and proliferation until embryonic day 13.5 and then enter mitotic arrest.[1] At postnatal day (PN) 1–2, gonocytes reenter the mitotic cycle and migrate to the periphery of the testicular cords; at PN 3–5, they give rise to spermatogonial stem cells (SSCs).[2–4] SSCs are present as single cells (A_s) that proliferate to renew the stem cell pool and produce undifferentiated spermatogonia (A_{pr} and A_{al}).[5] A_{al} spermatogonia then differentiate into A_1 spermatogonia, which undergo five rounds of cell division to form differentiated B spermatogonia that differentiate into preleptotene spermatocytes.[6] Preleptotene spermatocytes undergo one round of DNA duplication and two rounds of meiosis to form haploid spermatids, which then undergo a complicated metamorphosis involving nuclear structural modifications, acrosome formation, and flagellum establishment to become morphologically complete spermatozoa.[7–9]

The maintenance of the balance between spermatogonial proliferation and differentiation, and the initiation of spermatocyte meiosis, is vital for spermatogenesis that is regulated by a plethora of proteins. Extrinsic growth factors, including glial cell line-derived neurotrophic factor (Gdnf), epidermal growth factor (Egf), leukemia inhibitory factor (Lif), fibroblast growth factor 2 (Fgf2), colony-stimulating factor 1 (Csf1), insulin-like growth factor 1 (Igf1), and bone morphogenetic protein 4 (Bmp4), cause upregulation of the expression of many genes, such as promyelocytic leukemia zinc finger (*Plzf*), LIM homeobox protein 1 (*Lhx1*), ets variant 5 (*Etv5*), and B cell CLL/lymphoma 6-member B (*Bcl6B*), which support spermatogonial self-renewal and proliferation.[10] On the other hand, some factors, such as retinoic acid (RA) and stem cell factor (Scf), upregulated the KIT proto-oncogene and receptor tyrosine kinase (*Kit*), spermatogenesis- and oogenesis-specific basic helix-loop-helix 1/2 (*Sohlh1/2*), and stimulated by retinoic acid gene 8 (*Stra8*) gene expressions to suppress the proliferation signals and trigger spermatogonial differentiation.[11]

[1]School of Pharmaceutical Sciences, State Key Laboratory of Cellular Stress Biology, Xiamen University, Xiamen 361005, China; [2]Fujian Provincial Key Laboratory of Reproductive Health Research, Medical College of Xiamen University, Xiamen 361005, China; [3]Fujian Provincial Key Laboratory of Innovative Drug Target Research, School of Pharmaceutical Sciences, Xiamen 361005, China; [4]Department of Pathology, Division of Biological Sciences, University of California at San Diego, La Jolla, CA 92093, USA; [5]Ministry of Education Key Laboratory of Model Animals for Disease Study, Model Animal Research Center and Medical School of Nanjing University, National Resource Center for Mutant Mice, Nanjing 210061, China.
*These authors contributed equally to this work.
Correspondence: Dr. ZX Lu (zhongxian@xmu.edu.cn) or Dr. W Liu (w2liu@xmu.edu.cn)
Received: 30 November 2018; Accepted: 19 March 2019

In spermatogonia, a number of cytoplasmic signaling proteins, including phosphoinositide-3 kinase (Pi3k), protein kinase B (Akt/PKB), rat sarcoma viral oncogene (Ras), mitogen-activated protein kinase (Mapk), and mammalian target of rapamycin (mTOR), orchestrate these signals to maintain the spermatogonial proliferation/differentiation balance and proper differentiation.[12,13] In male mice, RA signaling induces the production of proteins through Stra8 and Kit, which activates germ cell differentiation and initiates meiosis.[14] In addition to the classical nuclear receptor signaling pathway, RA also activates Pi3k/Akt or Ras/extracellular-regulated protein kinase (Erk) signaling cascades to stimulate the expression of meiotic genes, such as disrupted meiotic cDNA 1 (*Dmc1*), REC8 meiotic recombination protein (*Rec8*), and synaptonemal complex protein 3 (*Sycp3*),[15] which form a series of meiotic structures that are responsible for the drastic morphologic changes of chromosomes during meiosis.[16]

Src homology domain tyrosine phosphatase 2 (Shp2), a nonreceptor tyrosine phosphatase encoded by the protein tyrosine phosphatase, nonreceptor type 11 (*Ptpn11*) gene, plays an important role in organ development by regulating multiple intracellular signaling pathways, notably the Ras/Erk Mapk, Janus kinase/signal transducer and activator of transcription 3 (Jak/Stat3), and Pi3k/Akt cascades.[17–20] Shp2 is expressed in testicular somatic cells and germ cells.[21] Our previous work demonstrated that conditional knockout of *Shp2* in Sertoli cells in mice leads to an upregulation of Scf signaling, resulting in premature differentiation of SSCs.[22] Puri *et al*.[23] showed that *Shp2* deletion in gonocytes (prospermatogonia) in mice, using DEAD (Asp-Glu-Ala-Asp) box polypeptide 4 (*Vasa*)-*cre*, severely impaired the transition of gonocytes into SSCs and led to the loss of undifferentiated spermatogonia in postnatal testes. However, the effect of Shp2 on later spermatogonial functions was not revealed. We and other researchers have also observed that Shp2 protein levels are high in spermatogonia but drop to low levels in spermatocytes and spermatids,[21] suggesting that Shp2 has a specific role in the differentiation of spermatogonia and the initiation of spermatocyte meiosis.

To elucidate the role of Shp2 in the transition from spermatogonia to spermatocytes, we deleted *Shp2* in postnatal germ cells in mice using the *Stra8-cre* model and found that spermatogenesis was disturbed. The proliferation/differentiation balance in mutant spermatogonia was disrupted, and differentiation was accelerated. *Shp2* deletion in spermatocytes also suppressed the expression of functional meiotic genes, which disturbed meiosis and ultimately led to spermatocyte loss.

MATERIALS AND METHODS

Transgenic mouse breeding and reproductive ability test

Mice were housed under standard conditions and had free access to food and water. All experimental procedures were performed according to the approved guidelines from the Animal Welfare Committee of Research Organization (X200811) of Xiamen University (Xiamen, China). All animal experiments conducted as part of this study were approved by the Animal Ethics Committee of Xiamen University. To generate the postnatal germ cell-specific *Shp2* conditional knockout mice, *Shp2^f/f* mice were bred with *Stra8-cre* mice. To increase the efficiency of *Shp2* deletion, *Stra8-cre-Shp2^f/null* F2 mice were generated and used as germ cell-specific *Shp2* knockout (GCKO) mice, and *Shp2^f/null* mice served as control mice. The genotype of offspring was confirmed by PCR using gene-specific primers (**Supplementary Table 1**).

To assay reproductive ability, adult 8-week-old GCKO, *Shp2^f/null* and *Shp2^f/f* male mice from the same litter were grouped and mated with wild-type female mice. On the second day, female mice with vaginal plugs were moved into another cage and observed until the pups were born. One week later, male mice were again mated with

other wild-type female mice. The mating experiment was successively repeated ten times for each male mouse. The number of litters and pups was statistically analyzed.

Isolation and purification of primary germ cells

Germ cell mixtures were isolated by a two-step enzymatic digestion as described previously.[24] Germ cells from the testes of 7-day-old (for the isolation of spermatogonia) and 17-day-old control males (for the isolation of preleptotene and leptotene/zygotene spermatocytes) were isolated by gravity sedimentation with a STA-PUT device (56700-012, ProScience, Toronto, Canada) and characterized from cytological classification and morphology analysis as described previously.[25] The purity of each germ cell population was confirmed by the expression of marker genes and morphology (**Supplementary Figure 1**). In general, more than 90% purity was achieved.

Quantitative real-time polymerase chain reaction (qRT-PCR)

Total mRNA was isolated from testes or separated germ cells by TRIzol reagent (Invitrogen, Waltham, MA, USA). cDNAs were produced with an PrimeScript™ II 1st Strand cDNA Synthesis Kit (TAKARA, Tokyo, Japan) following the standard manufacturer's instructions. qRT-PCR was performed in an ABI 7500 PCR system (Applied Biosystems, Foster City, CA, USA). Primer information is presented in **Supplementary Table 1**, and mRNA expression levels were normalized to glyceraldehyde-3-phosphate dehydrogenase (GAPDH) levels to determine the relative expression levels of genes.

Histology and immunohistochemistry

Testes were first fixed with 3.7% (*w*/*v*) formaldehyde (Solarbio® Life Sciences, Beijing, China) in PBS (pH 7.4) and then embedded in paraffin. Tissue sections (5 μm) were prepared and stained with hematoxylin and eosin (H and E; ZSbio, Beijing, China). For immunohistochemistry, tissue sections were incubated in antigen unmasking solution (ZSbio), deparaffinized, rehydrated, and incubated overnight at 4°C with primary antibodies, anti-Acvr1 (1:500, Santa Cruz Biotechnology, Santa Cruz, CA, USA). After being washed in PBS, the sections were incubated with horseradish peroxidase (HRP)-conjugated secondary antibody (ZSbio). The 3,3'-diaminobenzidine (DAB) colorimetric reagent (ZSbio) was added for 5 min as the substrate of HRP, and the sections were then counterstained in hematoxylin, dehydrated, cleared, and mounted.

Spermatocyte nuclear spreading

Nuclear spreading of spermatocytes was performed as described previously.[26] In brief, approximately 50 μl testicular or purified spermatocyte suspension was placed on a glass slide and mixed with 250 μl 1% (*v*/*v*) Triton X-100 (Solarbio® Life Sciences) in PBS. Spermatocyte swelling and spreading were monitored by phase-contrast microscopy (Primo Vert, Zeiss, Oberkochen, Germany). When cells obtained an opaque appearance, 300 μl fixative solution (3.7% [*w*/*v*] formaldehyde and 0.1 mol l⁻¹ sucrose, pH 7.4) was added to the slide and gently mixed by tilting. Slides were then air dried at 37°C and stored at −20°C until used.

Immunofluorescence staining

The prepared sections were blocked with 3% (*w*/*v*) bovine serum albumin (BSA; ZSbio) in PBST (0.1% [*v*/*v*] Triton X-100 in PBS) for 1 h at room temperature and then incubated with the following primary antibodies overnight at 4°C: anti-Sycp3 (1:200, Abcam, Cambridge, MA, USA), anti-synaptonemal complex protein 1 (Sycp1; 1:200, Abcam), anti-Vasa (1:500, Abcam), anti-c-kit (1:500, Abcam),

anti-Shp2 (1:200, Santa Cruz Biotechnology), anti-Plzf (1:500, Santa Cruz Biotechnology), anti-cleaved caspase 3 (1:200, Cell Signaling Technology, Boston, MA, USA), anti-Dmc1 (1:200, Abcam), anti-Smc3 (1:500, Abcam), and anti-DNA repair recombinase rad51 (Rad51; 1:200, Invitrogen). After being washed three times with PBST, the samples were incubated with the following secondary antibodies at a 1:200 dilution for 1 h at 37°C: Alexa Fluor 594/488-labeled anti-rabbit or anti-mouse IgG (YEASEN, Shanghai, China). The slides were subsequently washed three times in PBST and mounted with Vectashield containing 4'-6-diamidino-2-phenylindole (DAPI; Vector Laboratories, Burlingame, CA, USA).

TdT-mediated dUTP Nick-End Labeling (TUNEL) assay
Tissue sections were prepared as described above and were treated with 0.1% (*v/v*) Triton X-100 in 0.1% (*w/v*) sodium citrate solution for 10 min at 37°C and stained with the *in situ* Cell Death Detection Kit (Roche Applied Science, Basel, Switzerland) according to the manufacturer's protocol. Finally, the sections were incubated with Vectashield containing DAPI.

GC-1 cell line culture and treatment
Mouse-derived GC-1 cells (a gift from Dr. Fei Sun, Nantong University, Nantong, China) were cultured in Dulbecco's Modified Eagle Medium (DMEM; Gibco, Grand Island, CA, USA) supplemented with 10% (*v/v*) fetal bovine serum (FBS; Gibco). To knock down *Shp2*, the cells were infected with a high titer of lentivirus expressing Shp2 shRNA for 48 h, as described previously.[27] For retinoic acid (RA; Sigma-Aldrich, Saint Louis, MO, USA) treatment, the cells were incubated for the indicated times in medium containing 0.2% FBS and 3 μmol l^{-1} RA which is dissolved in dimethyl sulfoxide (DMSO).

Western blot
Western blot was performed as previously described.[22] In brief, separated proteins on nylon membranes were incubated with specific primary antibodies such as anti-Shp2 (1:1000) and anti-tubulin (1:1000, Proteintech, Wuhan, China) at 4°C overnight and then with secondary antibodies (ZSbio) at 37°C for 2 h. The results were visualized with enhanced chemiluminescence. Grayscale bands were quantified using Quantity One software (Bio-Rad, Hercules, CA, USA).

Statistical analysis
Statistical analysis was performed using GraphPad prism version 6.0 (GraphPad Software Inc., La Jolla, CA, USA). Data were presented as mean ± standard deviation (s.d.) and were analyzed by Student's *t*-test. $P < 0.05$ was considered statistically significant.

RESULTS
Deletion of Shp2 and its effect on spermatogenesis and fertility
In mouse testicular tissue or purified cells, Shp2 protein was abundant in spermatogonia and Sertoli cells but decreased to low levels in meiotic cells such as spermatocytes and spermatids (**Supplementary Figure 2**).

To define the role of Shp2 in the early stages of spermatogenesis, we employed *Stra8-cre* to delete the *Shp2* gene in male germ cells. *Stra8-cre* activity is restricted to the postnatal male germline, where it is detectable in undifferentiated spermatogonia in a few days after birth.[28] Here, we produced a *Stra8-cre-Shp2$^{f/null}$* F2 generation as GCKO mice and used *Shp2$^{f/null}$* mice as the control. Immunofluorescence analysis revealed that Shp2 was efficiently and specifically deleted in postnatal spermatogenic cells in juvenile GCKO mice (3-week-old) (**Figure 1a**, green), although Shp2 ablation efficiency decreased with age (**Supplementary Figure 3**, red).

Although the mutant mice had a normal body weight, their testes were smaller than those of control mice at various ages (**Figure 1b** and **1c**). Histological changes in testis tissue were observed with H and E staining. In 2–3-week-old juvenile control mice, the germ cells showed a regular arrangement, and spermatogenic development was clearly observed in the seminiferous tubules (**Figure 1d**, top panels). However, in GCKO mice of the same age, spermatogenic development was impaired, and germ cells were markedly decreased in number and disorderly arranged in most of seminiferous tubules in the testes from GCKO mice in particular, spermatids were nearly undetectable (**Figure 1d**, bottom panels). The defective spermatogenetic phenotype was also observed in many seminiferous tubules in the testes from 4- to 8-week-old GCKO mice. However, spermatogenesis in some seminiferous tubules recovered in older mice (**Supplementary Figure 4a**).

Adult GCKO and age-matched control male mice (*Shp2$^{f/null}$*) were mated with wild-type females beginning at 8-week-old to perform a successive breeding assay (see details in the Methods section). In a total of 96 matings, the GCKO male mice (*n* = 8) sired a total of 310 pups (68 litters), while control mice (*n* = 7) sired a total of 461 pups from 67 litters. The average number of pups per litter from GCKO mice was lower than that from control mice ($P < 0.01$; **Supplementary Table 2**). In addition, the number of spermatids was dramatically decreased in adult GCKO mice, as visualized by Acvr1 (a spermatid marker protein; **Supplementary Figure 4b**) and DNA content analysis with flow cytometry (**Supplementary Figure 4c** and **4d**). Approximately half (48%) of all pups from *Stra8-cre-Shp2$^{f/null}$* (GCKO) male mice were *Shp2* positive (F/+) rather than the theoretically expected *Shp2* heterozygous (null/+) genotype (**Supplementary Table 3**).

The effect of Shp2 deletion on spermatogonial differentiation
To understand the spermatogenetic defect due to Shp2 ablation, we first discovered the effect of Shp2 deletion on the balance between undifferentiated spermatogonia proliferation and differentiation. Plzf is an undifferentiated spermatogonia marker protein,[29] and the number of Plzf-positive spermatogonia was reduced in 7-day-old GCKO mice by both immunostaining and qRT-PCR analyses (**Figure 2a, 2b** and **Supplementary Figure 5**). Loss of Shp2 also suppressed the expression of *Etv5* and *Bcl6B* (**Figure 2b**, qRT-PCR), two genes activated by Gdnf and Fgf signalings that play key roles in maintaining the balance between spermatogonia self-renewal and proliferation. In addition, the number of phosphorylated histone H3 (PH3; a cell proliferation marker[30]) positive undifferentiated spermatogonia (PH3$^+$, Plzf$^+$) was also reduced in the testes from GCKO mice (**Figure 2c** and **Supplementary Figure 5**). c-Kit is a marker of differentiating spermatogonia, and *c-Kit* gene transcription in postnatal germ cells is concordant with the first appearance of differentiating spermatogonia, which occurs at approximately PN7 in mice.[31] Here, although c-Kit was expressed at low levels in a few spermatogonia from control mice, it was highly expressed in many spermatogonia in GCKO mice (**Figure 2d** and **Supplementary Figure 5**) at PN7. The mRNA levels of *c-Kit* and deleted in azoospermia like (*Dazl*) were also upregulated in Shp2-depleted testes from 7-day-old GCKO mice, while SRY-box 3 (Sox3) transcription was not affected (**Figure 2e**).

The effect of Shp2 deletion on spermatocyte meiosis and death
We observed spermatocyte meiosis by immunofluorescence staining with Sycp1 and Sycp3, which are components of the germ cell-specific synaptonemal complex (SC).[32] In control mice, Sycp3 expression was
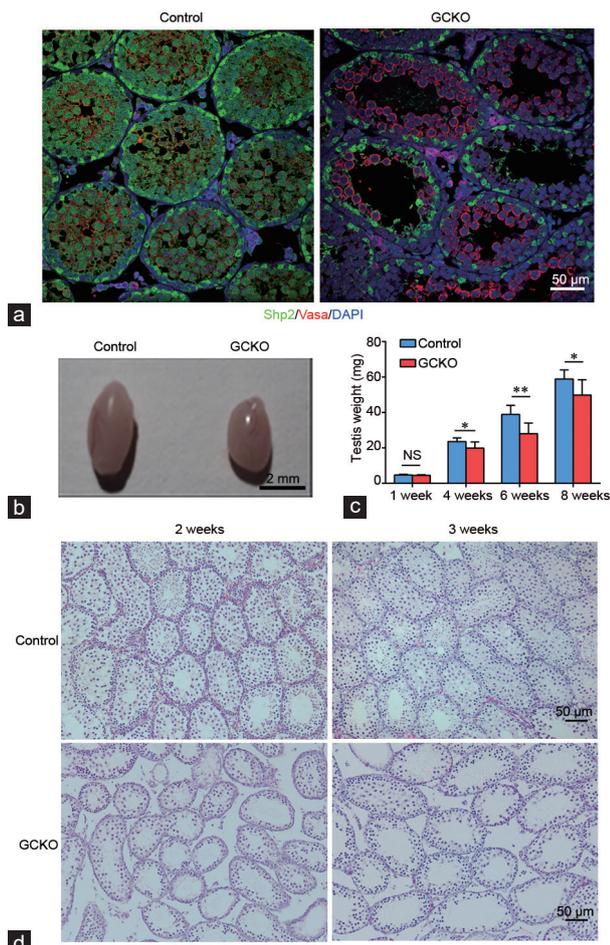
Figure 1: The effect of Shp2 ablation in male germ cells on testicular function and male infertility test. (**a**) Evaluation of Shp2 deletion by immunofluorescence staining in germ cells in the seminiferous tubules from 3-week-old control (*Shp2^f/null*) and germ cell conditional *Shp2* knockout (GCKO) mice. Tissue sections were stained with Shp2 (green), Vasa (red), and DAPI (blue). Multiple photographs were taken, and representative images are presented. Scale bar = 50 μm. (**b**) Testes from *Shp2^f/null* and GCKO male mice at 4 weeks. Scale bar = 2 mm. (**c**) The average weight of the testes from 1- to 8-week-old control and GCKO mice is shown in columns. The values are expressed as the mean ± s.d. from eight mice. Statistical analysis was performed with Student's *t*-test. Asterisks denote statistical significance; *P < 0.05 and **P < 0.01. (**d**) Histological structure of testes from 2- and 3-week-old *Shp2^f/null* and GCKO mice as shown by H and E staining. Multiple photographs were taken, and representative images are presented. Scale bars = 50 μm. Control: control mice; GCKO: germ cell-specific *Shp2* knockout mice; Shp2: Src homology domain tyrosine phosphatase 2; V1AD (Asp-Glu-Ala-Asp) box polypeptide 4; DAPI: 4'-6-diamidino-2-phenylindole; s.d: standard deviation; NS: not significant; H and E: hematoxylin and eosin.

low in preleptotene spermatocytes located in the basal compartment of seminiferous tubules at PN8 to PN10 and became strong and thread-like in leptotene and zygotene spermatocytes, which clustered into the adluminal compartment of seminiferous tubules at PN11 to PN13 (**Figure 3a**, top panels). Sycp1 expression was first noted in zygotene spermatocytes and was high in pachytene spermatocytes. Here, Sycp1 was coexpressed with Sycp3 at PN14 in spermatocytes (**Figure 3a**, top panels). In GCKO mice, leptotene and zygotene spermatocytes appeared at PN9 (**Figure 3a**, bottom panels), and only a few pachytene spermatocytes were observed at PN11–13 (**Figure 3a**, bottom panels), indicating abnormal spermatocyte meiosis.
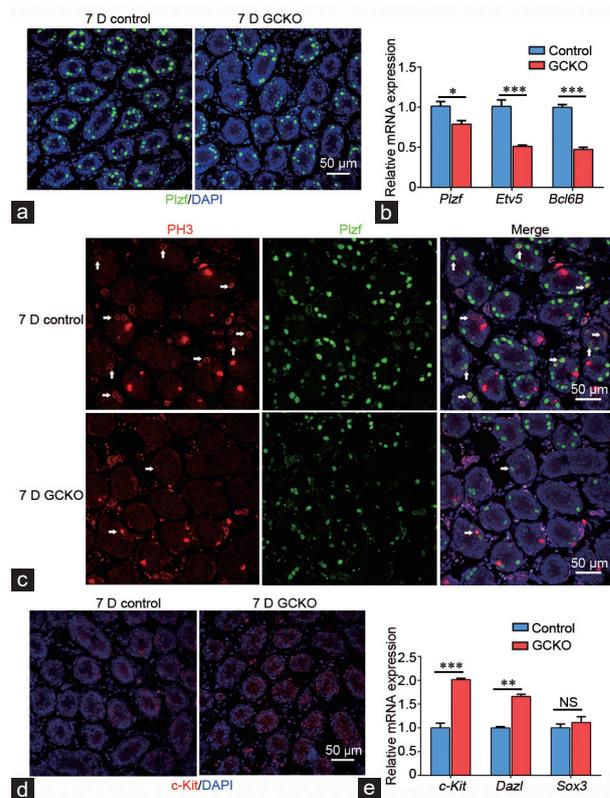

Figure 2: Shp2 deletion and spermatogonial differentiation. (**a**) Immunofluorescence staining of Plzf in the testicular tissue from 7-day-old mice (green). DAPI is the control (blue). Multiple photographs were taken, and representative images are presented. (**b**) qRT-PCR analysis of the expression of spermatogonial proliferation genes in the testes of 7-day-old control and GCKO mice. Gene expression is presented as the fold change compared with that in control mice after normalization to GAPDH. Data are presented as the mean ± s.d. of three separate experiments. *P < 0.05 and ***P < 0.001. *Plzf*, *Etv5*, and *Bcl6B* expression levels were compared between control and GCKO testes. (**c**) Co-immunofluorescence staining of PH3 (red) and Plzf (green) in the testicular tissue from 7-day-old mice. Multiple photographs were taken, and representative images are presented. DAPI is the control (blue). The white arrowheads indicate PH3- and Plzf-positive cells. (**d**) Immunofluorescence staining for c-Kit in the testis tissue from 7-day-old mice (red). Multiple photographs were taken, and representative images are presented. DAPI is the control (blue). (**e**) qRT-PCR analysis of the expression of spermatogonial differentiation genes in the testes of 7-day-old control and GCKO mice. **P < 0.01 and ***P < 0.001. *Dazl*, *c-Kit*, and *Sox3* expression levels were compared between control and GCKO testes. Scale bars = 50 μm. Control: control mice; GCKO: germ cell-specific *Shp2* knockout mice; *Plzf*: promyelocytic leukemia zinc finger; *Etv5*: ets variant 5; *Bcl6B*: B cell CLL/lymphoma 6, member B; PH3: Phosphorylated histone H3; *c-Kit*: KIT proto-oncogene and receptor tyrosine kinase; *Dazl*: deleted in azoospermia like; *Sox3*: SRY-box 3; DAPI: 4'-6-diamidino-2-phenylindole; D: days; qRT-PCR: quantitative real-time polymerase chain reaction; NS: not significant; s.d.: standard deviation.

In addition, although not all the tubules were completely affected as described above, the number of meiotic cells was dramatically decreased in GCKO mice compared with that in control mice (**Figure 3b**). In GCKO mice, cell apoptosis occurred at PN9 and increased notably starting at PN10 (**Figure 4a** and **4b**). These apoptotic cells were scattered in the adluminal compartment of seminiferous tubules (**Figure 4a**, bottom panel). Moreover, cleaved caspase 3 levels were markedly increased in GCKO mice from PN10, which confirmed the observation of spermatocyte death induced by Shp2 deficiency (**Supplementary Figure 6**).
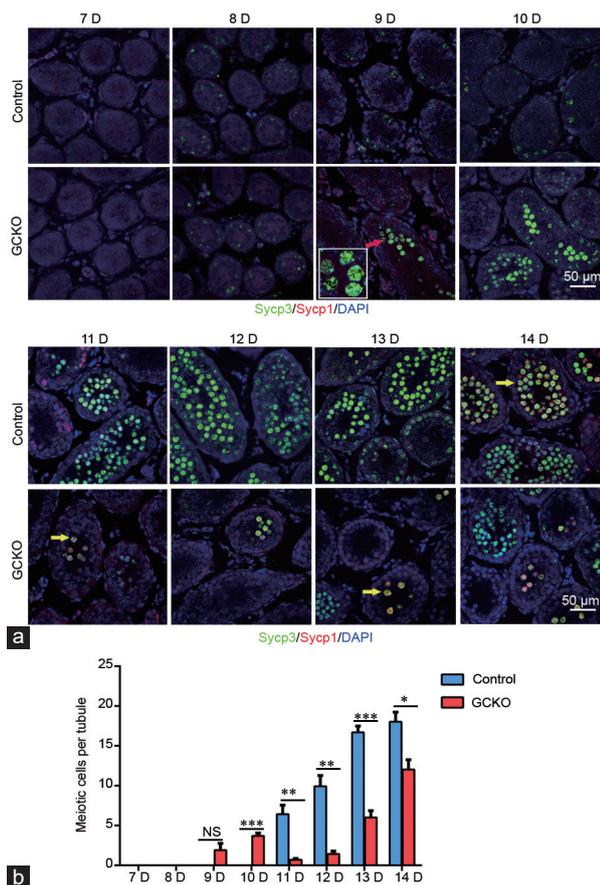
Figure 3: The effect of Shp2 deletion on the progression of spermatocyte meiosis. (**a**) Immunofluorescence staining of meiotic spermatocytes from mice at different ages. Spermatocytes from 7- to 14-day-old control (*Shp2^f/null*) and GCKO mice were stained for Sycp1 (red), Sycp3 (green), and DAPI (blue). Red and yellow arrowheads indicate meiotic leptotene/zygotene and pachytene spermatocytes, respectively. Multiple photographs were taken, and representative images are presented. Scale bars = 50 μm. (**b**) Quantification of meiotic cells per tubule in the testes sections from control (*Shp2^f/null*) and GCKO mice. Data are presented as the mean ± s.d. of at least five mice from different litters. *P < 0.05; **P <0.01 and ***P < 0.001. Meiotic cells per tubule in the testes sections were compared between control and GCKO testes at same time point. Control: control mice; GCKO: germ cell-specific *Shp2* knockout mice; Sycp3: synaptonemal complex protein 3; Sycp1: synaptonemal complex 1; DAPI: 4'-6-diamidino-2-phenylindole; D: days; NS: not significant; s.d.: standard deviation.

Figure 4: The effect of Shp2 deletion on germ cell apoptosis. (**a**) Cell apoptosis analysis of testis tissue from 7- to 14-day-old control and GCKO mice with TUNEL assays (green color). Sycp3 (red) is a meiotic spermatocyte marker. Multiple photographs were taken, and representative images are presented. Scale bars = 50 μm. (**b**) Quantification of the number of TUNEL-positive cells per tubule on the transverse tubule sections of the testes. The cell nucleus was stained with DAPI. The values are expressed as the mean ± s.d. from at least five mice from different litters. Statistical analysis was performed using Student's *t*-test. Asterisks denote statistical significance. **P < 0.01 and ***P < 0.001. TUNEL-positive cells per tubule in the testes sections were compared between control and GCKO testes at same time point. Control: control mice; GCKO: germ cell-specific *Shp2* knockout mice; Sycp3: synaptonemal complex protein 3; TUNEL: TdT-mediated dUTP nick-end labeling; DAPI: 4'-6-diamidino-2-phenylindole; D: days; NS: not significant.

The expression of meiotic genes and meiotic structure formation in Shp2-ablated spermatogenic cells

To explore the mechanism underlying the meiosis defection, meiotic genes' expressions in spermatogonia (SG), preleptotene spermatocytes (PlpSC), and leptotene/zygotene spermatocytes (L/ZSC) from control and GCKO mice were measured by qRT-PCR. The expressions of several genes involved in meiotic recombination, such as initiator of meiotic double-stranded breaks (*Spo11*), PR domain containing 9 (*Prdm9*), *Dmc1*, *Rad51*, and mutS homolog 4 (*Msh4*), and of genes involved in meiotic synapses, such as *Sycp1, Sycp3,* synaptonemal complex central element protein 2 (*Syce2*), structural maintenance of chromosomes 3 (*Smc3*), and stromal antigen 1 (*Stag1*), were attenuated in preleptotene spermatocytes from GCKO mice compared to those from control mice (**Figure 5a**).

We evaluated the impact of meiotic protein deficiency by performing nuclear spreading assays with immunofluorescence staining of several marker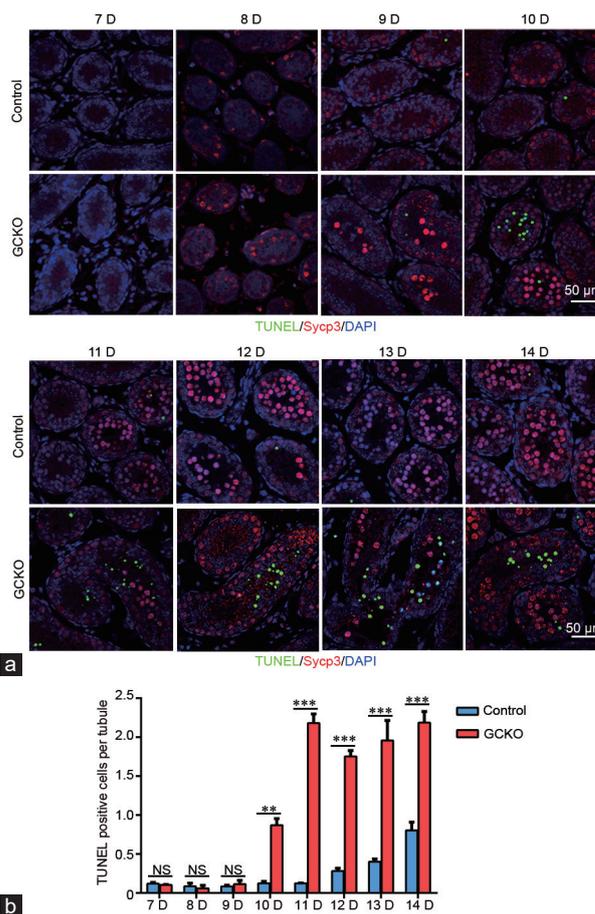 proteins. Dmc1 forms early recombination nodules (ENs) with Rad51 to repair meiotic double-strand breaks (DSBs) by homologous recombination.[33,34] In control spermatocytes, Rad51/Dmc1 formed ENs along the axial elements (AEs), starting from the leptotene stage, and the number of these complexes gradually decreased with maturation (**Figure 5b**). However, in GCKO spermatocytes, Rad51 expression appeared to be normal at the leptotene stage but completely absent at the zygotene stage, and Dmc1 was undetectable at any of these stages (**Figure 5b**). Smc3, a cohesion protein that forms the central element of the synaptonemal complex (SC) with other proteins,[35] was localized along the entire SC in control leptotene and zygotene spermatocytes, but was completely absent when Shp2 was deleted (**Figure 5b**).

Knockdown of Shp2 and its effect on RA signaling and target gene expression

RA is an important signal for initiating meiosis and inducing meiotic gene expression.[36,37] In addition to the classical nuclear receptor
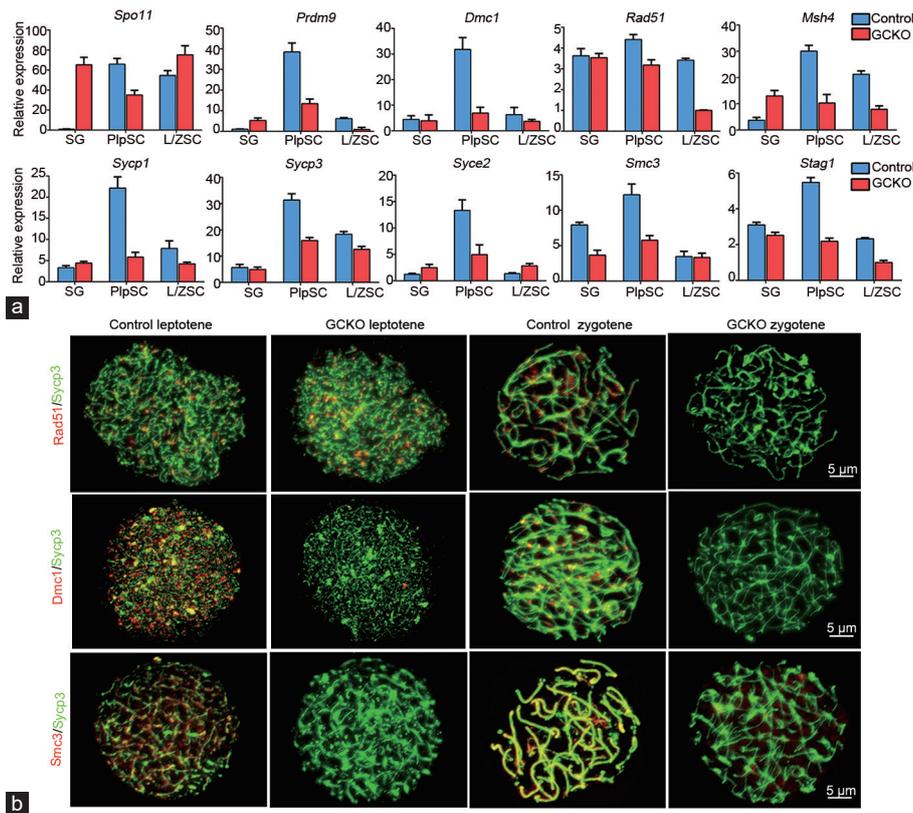
Figure 5: The expression of meiotic genes and meiotic structure formation in Shp2-ablated spermatogenic cells. (**a**) qRT-PCR analysis of meiotic genes in isolated spermatogenic cells at different stages as indicated. Gene expression is presented as the fold change compared to control mice after normalization to GAPDH. Data are presented as the mean ± s.d. of three separate experiments. (**b**) Meiotic events were evaluated by nuclear spreading and immunofluorescence analysis. Leptotene and zygotene spermatocytes were stained for Sycp3 (green) or Rad51 (red, top row), Dmc1 (red, middle row), and Smc3 (red, bottom row). Multiple photographs were taken, and representative images are presented. Scale bars = 5 μm. SG: spermatogonia; PlpSC: preleptotene spermatocytes; L/ZSC: leptotene/zygotene spermatocytes; Control: control mice; GCKO: germ cell-specific *Shp2* knockout mice; *Spo11*: initiator of meiotic double-stranded breaks; *Prdm9*: PR domain containing 9; *Dmc1*: DNA meiotic recombinase 1; *Rad51*: DNA repair recombinase rad51; *Msh4*: mutS homolog 4; *Sycp1*: synaptonemal complex protein 1; *Sycp3*: synaptonemal complex protein 3; *Syce2*: synaptonemal complex central element protein 2; *Smc3*: structural maintenance of chromosomes 3; *Stag1*: stromal antigen 1; qRT-PCR: quantitative real-time polymerase chain reaction; GAPDH: glyceraldehyde-3-phosphate dehydrogenase; s.d.: standard deviation.

signaling pathway, RA also activates the Pi3k/Akt or Ras/Erk signaling cascade to stimulate meiotic gene expression.[15] As a crucial regulator of the Pi3k/Akt and Ras/Erk pathways, Shp2 might also regulate RA signaling through these cytoplasmic signaling pathways. To assess this hypothesis, *Shp2* was specifically knocked down in GC-1 cells, a germ cell line that corresponds to a stage between B type spermatogonia and primary spermatocytes,[38] with lentivirus containing plasmid expressing short hairpin RNA targeting Shp2 (sh-Shp2) or control (shN). Shp2 protein levels were obviously decreased (by more than 60%) in GC-1 cells infected with sh-Shp2 lentivirus (**Figure 6a**). Then, we checked the expressions of meiotic genes (*Sycp3* and *Dmc1*) after 48 h of RA treatment by qRT-PCR and found that Shp2 knockdown downregulated RA-stimulated meiotic gene expression in GC-1 cells (**Figure 6b**). Furthermore, the cells were stimulated with 3 μmol l^{-1} RA for 15 min, and Akt and Erk phosphorylation was checked by Western blot with specific antibodies. The results showed that RA increased Akt and Erk signaling in GC cells, while Shp2 ablation impaired this effect, reducing the RA-induced phosphorylation of Akt and Erk (**Figure 6c** and **6d**).

DISCUSSION

By the use of conditional knockout mice, the present study demonstrated that loss of *Shp2* in postnatal germ cells leads to uncontrolled spermatogonial differentiation and defective spermatocyte meiosis, revealing a critical role of Shp2 in spermatogenesis.

Shp2 deletion in germ cells seriously impaired spermatogenesis in our animal model. Histological observations revealed that germ cells were markedly decreased in number and disorderly arranged in most seminiferous tubules in the testes from 2–3-week-old GCKO mice, and spermatids were nearly undetectable. Immunofluorescence staining also revealed that the spermatocyte population was sharply decreased, and cell apoptosis increased from PN10. Few pachytene spermatocytes were observed at PN11–13. These findings demonstrate that Shp2 is crucial for spermatogenesis and that germ cells lacking Shp2 are not able to develop into spermatids. In the breeding test of *Stra8-cre-Shp2*[f/null] (GCKO) male mice and wild-type female mice, approximately 50% of the pups were *Shp2* heterozygous (F/+), rather than the expected 100% *Shp2*[+/null] pups, which suggests that no spermatozoa were derived from *Shp2*[null/null] germ cells.

However, any incomplete Shp2 deletion with the *Stra8-cre* system would dilute the defect in spermatogenesis and weakened the GCKO mouse phenotype. Although *Stra8-cre* is a powerful tool for studying spermatogenesis that has been employed by several groups, it is well known that incomplete deletion in the *Stra8-cre* model disturbs the phenotype and brings much confusion for researchers.[39,40] The *Stra8-cre* deletion efficiency may be higher in undifferentiated spermatogonia
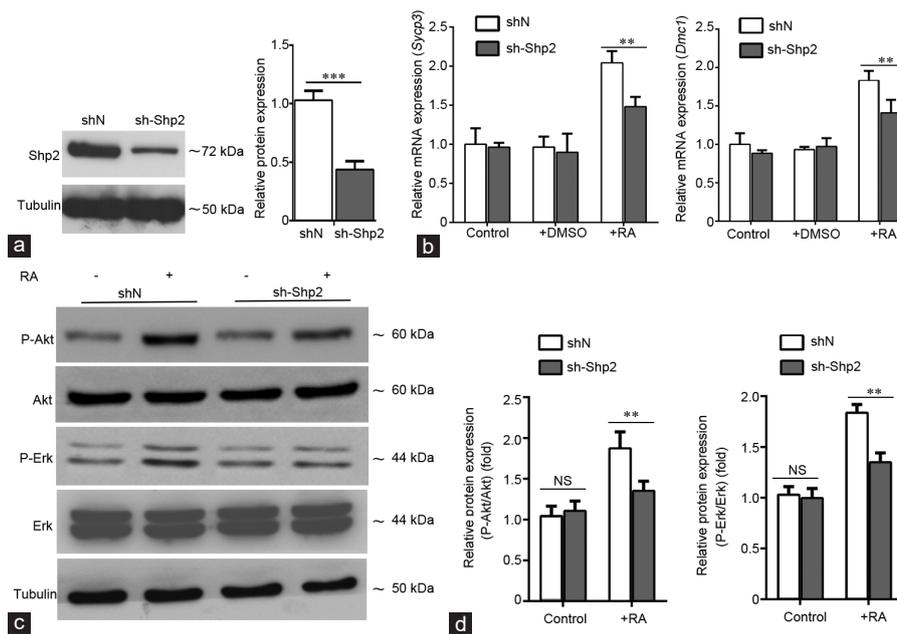
Figure 6: Knockdown of *Shp2* and its effect on retinoic acid signaling and target gene expression. (**a**) Shp2 protein level in GC-1 cells infected with lentivirus containing Shp2 shRNA (sh-Shp2) for 48 h was evaluated by Western blot. Tubulin was used as a loading control. The quantification of the results is shown on the right. Protein levels were normalized to tubulin levels ($n = 3$, ***$P < 0.001$). Shp2 protein levels were compared between shN and shRNA lentivirus infected GC-1 cells. (**b**) mRNA levels of the RA target genes *Sycp3* and *Dmc1* in GC-1 cells treated with 3 μmol l^{-1} RA for 48 h were measured by qRT-PCR. Data are shown as the mean ± s.d. ($n = 3$, **$P < 0.01$). *Sycp3* and *Dmc1* mRNA levels were compared between shN and shRNA lentivirus infected GC-1 cells. (**c**) The phosphorylation of Erk and Akt in GC-1 cells treated with or without 3 μmol l^{-1} RA for 15 min was determined by Western blot. Tubulin was used as a loading control. (**d**) Quantification of Erk and Akt phosphorylation as described in **b**. Protein levels were normalized to total Erk or Akt levels. Data are shown as the mean ± s.d. ($n = 3$, **$P < 0.01$). P-Erk and Erk relative protein levels were compared between shN and shRNA lentivirus infected GC-1 cells. NS: not significant; shN: lentivirus containing control plasmid; sh-Shp2: lentivirus containing plasmid expressing short hairpin RNA targeting Shp2; *Sycp3*: synaptonemal complex 3; *Dmc1*: DNA meiotic recombinase 1; Erk: extracellular regulated protein kinase; Akt: AKT serine/threonine kinase; P-Erk: phosphorylated Erk; P-Akt: phosphorylated Akt; qRT-PCR: quantitative real-time polymerase chain reaction; RA: retinoic acid; s.d.: standard deviation.

in juveniles and decrease to the minimum in spermatogonia in adult testes, in which only pachytene spermatocytes and spermatids show Cre activity.[41] In our model, Shp2 was efficiently and specifically deleted in postnatal spermatogenic cells in younger GCKO mice, but the Shp2 ablation efficiency decreased with age. Therefore, the spermatogenic defect phenotype was clear in the first cycle of spermatogenesis (at 3-week-old), but was weaker in the second and later spermatogenic waves.

Shp2 protein was abundant in spermatogonia, but its level sharply decreased in meiotic spermatocytes, indicating that Shp2 has various roles in spermatogenesis. Using *Vasa-cre*, our group[22] and Puri *et al*.[23] deleted the *Shp2* gene in mouse gonocytes (prospermatogonia) and demonstrated that Shp2 is an essential protein for the survival and self-renewal of SSCs. However, the role of Shp2 in later spermatogonia development was not revealed because the population of undifferentiated spermatogonia gradually decreased and completely disappeared by 3-week-old in *Vasa-cre*-induced *Shp2* knockout mice. Here, our experiments using the *Stra8-cre* mouse model complemented the research on *Shp2* in early spermatogenesis and showed that *Shp2* deletion in undifferentiated spermatogonia reduced proliferation and accelerated differentiation, indicating that Shp2 also plays a positive role in maintaining the balance between spermatogonial proliferation and differentiation and that its proper withdrawal is beneficial to spermatogonial differentiation.

Shp2 also plays important physiological roles in the development of several other organs, such as the heart, pancreas, liver, and mammary gland, as a signaling protein that regulates the balance between proliferation and differentiation in progenitor stem cells.[42–44] In these tissues, Shp2 plays dual roles in regulating several signaling factors, such as Fgf, Gdnf, Egf, and Scf, which balance proliferation and differentiation.[45–47] As a typical protein tyrosine phosphatase (PTP), Shp2 dephosphorylates receptor tyrosine kinases (RTKs) and suppresses these signals. On the other hand, Shp2 can also enhance these signals to activate the downstream cytoplasmic signaling proteins Erk and Akt by dephosphorylating these proteins' activators (such as Src family kinases) or inhibitors (such as Sprouty, RasGAP).[18] In spermatogenesis, these RTK signals balance spermatogonia proliferation and differentiation.[7,10] Therefore, in spermatogonia, Shp2 may act as a gatekeeper to govern the balance between self-renewal and differentiation by orchestrating multiple signaling pathways, and its withdrawal induces unlimited spermatogonial differentiation.

In normal mouse spermatogenesis, undifferentiated spermatogonia differentiate into preleptotene spermatocytes at approximately PN8.[48] These spermatocytes reach the leptotene stage at approximately PN10 and the pachytene stage at PN14–16 in the mouse, depending on the strain.[2,49–51] In our transgenic mice, spermatocyte meiosis was initiated at PN11 and reached the pachytene stage at PN14 in control mice. However, in GCKO mice, leptotene and zygotene spermatocytes appeared at PN9, and pachytene-like spermatocytes emerged precociously at PN11, which indicated that meiosis was shifted earlier and shortened. Moreover, the spermatocyte population in GCKO mice was markedly decreased, and apoptosis appeared at PN9, suggesting that the disrupted meiosis in Shp2-deficient spermatocytes leads to cell death. Furthermore, we found that the expressions of many meiotic

genes in preleptotene spermatocytes were attenuated, which may be a main reason for the defects because meiosis depends on meiotic genes to form a series of structures that are responsible for the drastic morphological changes in chromosomes.[16] As evidence, the Rad51 and Dmc1 deficiency in Shp2-deleted spermatocytes led to the failed formation of early recombinant nodules in meiosis and a decrease in Smc3 disrupted SC formation.

The attenuation of meiotic gene expression may be due to disturbed meiotic progression. Spermatocytes require a long preleptotene stage to accumulate sufficient resources, especially functional meiotic proteins, for meiosis. A short or untimely preleptotene stage in spermatocytes may interrupt the transcription of meiotic genes. In addition, the loss of *Shp2* may impair the expression of meiotic genes. RA is a meiotic initiation signal that activates Stra8 and Dazl to induce the expression of meiotic genes, such as *Dmc1*, *Rec8*, and *Sycp3*.[15] Using GC-1 cells, a germ cell line with a stage between B type spermatogonia and primary spermatocytes,[38] we found that *Shp2* knockdown inhibited the RA-induced phosphorylation of Akt and Erk and the expression of meiotic genes *Sycp3* and *Dmc1*. Thus, Shp2 may also mediate the expression of meiotic genes by regulating RA signaling in spermatocytes.

Shp2 plays pleiotropic roles in human physiological processes and its dysfunction is involved in multiple of human developmental disorders and diseases.[17,18] Therefore, Shp2 is regarded as a potential therapeutic target. Gain-of-function mutations of the *Ptpn11* gene have been associated with Noonan syndrome and several cancers, including leukemia, lung, and breast cancer.[52–54] Allosteric inhibition of Shp2 has been demonstrated to be an effective therapeutic approach for cancer.[55] Lots of inhibitors of Shp2 activity have been identified as candidate drugs for cancer.[56,57] On the other hand, loss-of-function mutations of the *Ptpn11* gene have been previously identified, and these mutations result in several human developmental pathologies, such as LEOPARD syndrome, metachondromatosis, and hypertrophic cardiomyopathy.[58–60] Thus, activation of Shp2 is also thought to be a potential therapeutic approach for the treatment of human developmental disorders including infertility, although *Shp2* mutations and defects in infertility patients need to be further explored in the clinic.

CONCLUSION

High Shp2 protein levels are necessary for spermatogonia to maintain their self-renewal and survive, but spermatogonia differentiation requires the timely withdrawal of Shp2. In addition, low Shp2 levels play a role in spermatocyte meiosis by regulating RA-induced meiotic gene expression.

AUTHOR CONTRIBUTIONS

ZXL and WL participated in the design of the experiment and in the drafting and revision of the article. HBW guided the experiment directions. YL acquired, interpreted, and analyzed the data and drafted the manuscript. WSL bred transgene mice and participated in acquiring, interpreting and analyzing the data. JY, and JCD participated in the exploration of signaling pathways. SBK, YNZ, and YPT participated in the histology and IHC staining. CJL and GSF provided genetic mice, pointed out deficiencies, and amended the manuscript. All authors read and approved the final manuscript and agreed with the order of presentation of the authors.

COMPETING INTERESTS

All authors declared no competing interests.

REFERENCES

1 Western PS, Miles DC, van den Bergen JA, Burton M, Sinclair AH. Dynamic regulation of mitotic arrest in fetal male germ cells. *Stem Cells* 2008; 26: 339–47.
2 Bellve AR, Cavicchia JC, Millette CF, O'Brien DA, Bhatnagar YM, *et al*. Spermatogenic cells of the prepuberal mouse. Isolation and morphological characterization. *J Cell Biol* 1977; 74: 68–85.
3 Garcia TX, DeFalco T, Capel B, Hofmann MC. Constitutive activation of NOTCH1 signaling in Sertoli cells causes gonocyte exit from quiescence. *Dev Biol* 2013; 377: 188–201.
4 Yoshida S, Sukeno M, Nakagawa T, Ohbo K, Nagamatsu G, *et al*. The first round of mouse spermatogenesis is a distinctive program that lacks the self-renewing spermatogonia stage. *Development* 2006; 133: 1495–505.
5 de Rooij DG. Proliferation and differentiation of spermatogonial stem cells. *Reproduction* 2001; 121: 347–54.
6 de Rooij DG, Russell LD. All you wanted to know about spermatogonia but were afraid to ask. *J Androl* 2000; 21: 776–98.
7 Oatley JM, Brinster RL. Regulation of spermatogonial stem cell self-renewal in mammals. *Annu Rev Cell Dev Biol* 2008; 24: 263–86.
8 He Z, Kokkinaki M, Dym M. Signaling molecules and pathways regulating the fate of spermatogonial stem cells. *Microsc Res Tech* 2009; 72: 586–95.
9 Hermo L, Pelletier RM, Cyr DG, Smith CE. Surfing the wave, cycle, life history, and genes/proteins expressed by testicular germ cells. Part 1: background to spermatogenesis, spermatogonia, and spermatocytes. *Microsc Res Tech* 2010; 73: 241–78.
10 Kanatsu-Shinohara M, Shinohara T. Spermatogonial stem cell self-renewal and development. *Annu Rev Cell Dev Biol* 2013; 29: 163–87.
11 Mei XX, Wang J, Wu J. Extrinsic and intrinsic factors controlling spermatogonial stem cell self-renewal and differentiation. *Asian J Androl* 2015; 17: 347–54.
12 Song HW, Wilkinson MF. Transcriptional control of spermatogonial maintenance and differentiation. *Semin Cell Dev Biol* 2014; 30: 14–26.
13 Serra ND, Velte EK, Niedenberger BA, Kirsanov O, Geyer CB. Cell-autonomous requirement for mammalian target of rapamycin (Mtor) in spermatogonial proliferation and differentiation in the mousedagger. *Biol Reprod* 2017; 96: 816–28.
14 Busada JT, Geyer CB. The role of retinoic acid (RA) in spermatogonial differentiation. *Biol Reprod* 2016; 94: 10.
15 Pellegrini M, Filipponi D, Gori M, Barrios F, Lolicato F, *et al*. ATRA and KL promote differentiation toward the meiotic program of male germ cells. *Cell Cycle* 2008; 7: 3878–88.
16 Page SL, Hawley RS. The genetics and molecular biology of the synaptonemal complex. *Annu Rev Cell Dev Biol* 2004; 20: 525–58.
17 Grossmann KS, Rosario M, Birchmeier C, Birchmeier W. The tyrosine phosphatase Shp2 in development and cancer. *Adv Cancer Res* 2010; 106: 53–89.
18 Tajan M, de Rocca Serra A, Valet P, Edouard T, Yart A. SHP2 sails from physiology to pathology. *Eur J Med Genet* 2015; 58: 509–25.
19 Zhang SQ, Tsiaras WG, Araki T, Wen G, Minichiello L, *et al*. Receptor-specific regulation of phosphatidylinositol 3'-kinase activation by the protein tyrosine phosphatase Shp2. *Mol Cell Biol* 2002; 22: 4062–72.
20 Ke Y, Lesperance J, Zhang EE, Bard-Chapeau EA, Oshima RG, *et al*. Conditional deletion of Shp2 in the mammary gland leads to impaired lobulo-alveolar outgrowth and attenuated Stat5 activation. *J Biol Chem* 2006; 281: 34374–80.
21 Puri P, Walker WH. The tyrosine phosphatase SHP2 regulates Sertoli cell junction complexes. *Biol Reprod* 2013; 88: 59.
22 Hu X, Tang Z, Li Y, Liu W, Zhang S, *et al*. Deletion of the tyrosine phosphatase Shp2 in Sertoli cells causes infertility in mice. *Sci Rep* 2015; 5: 12982.
23 Puri P, Phillips BT, Suzuki H, Orwig KE, Rajkovic A, *et al*. The transition from stem cell to progenitor spermatogonia and male fertility requires the SHP2 protein tyrosine phosphatase. *Stem Cells* 2014; 32: 741–53.
24 Ogawa T, Arechaga JM, Avarbock MR, Brinster RL. Transplantation of testis germinal cells into mouse seminiferous tubules. *Int J Dev Biol* 1997; 41: 111–22.
25 Bellve AR. Purification, culture, and fractionation of spermatogenic cells. *Methods Enzymol* 1993; 225: 84–113.
26 Scherthan H, Jerratsch M, Li B, Smith S, Hulten M, *et al*. Mammalian meiotic telomeres: protein composition and redistribution in relation to nuclear pores. *Mol Biol Cell* 2000; 11: 4189–203.
27 Tao J, Zheng L, Meng M, Li Y, Lu Z. Shp2 suppresses the adipogenic differentiation of preadipocyte 3T3-L1 cells at an early stage. *Cell Death Discov* 2016; 2: 16051.
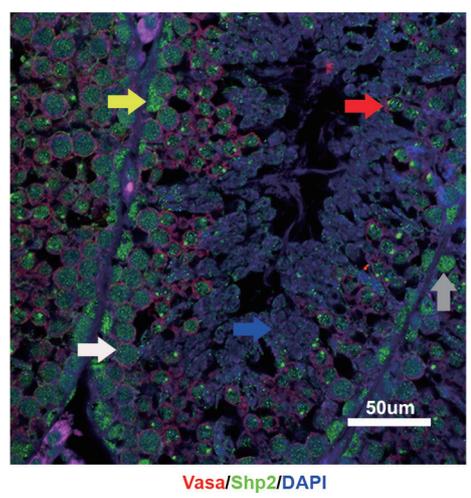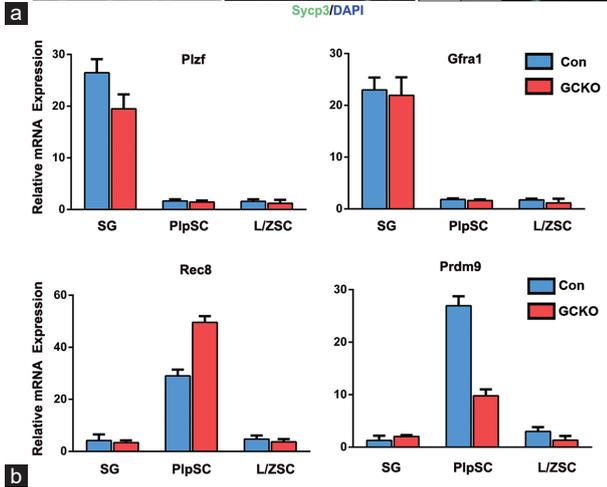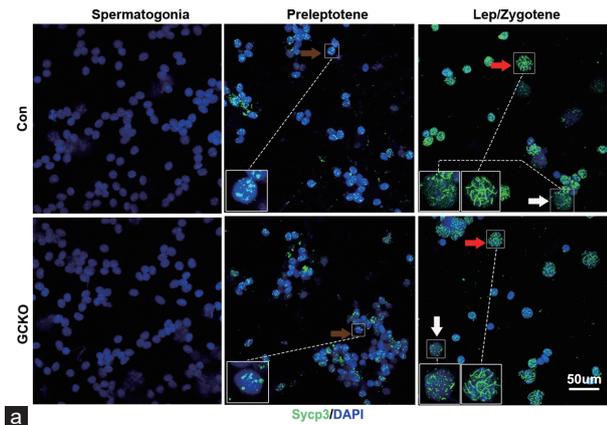
28 Sadate-Ngatchou PI, Payne CJ, Dearth AT, Braun RE. Cre recombinase activity specific to postnatal, premeiotic male germ cells in transgenic mice. *Genesis* 2008; 46: 738–42.

29 Costoya JA, Hobbs RM, Barna M, Cattoretti G, Manova K, *et al.* Essential role of Plzf in maintenance of spermatogonial stem cells. *Nat Genet* 2004; 36: 653–9.

30 Wilkens J, Williams AR, Chwalisz K, Han C, Cameron IT, *et al.* Effect of asoprisnil on uterine proliferation markers and endometrial expression of the tumour suppressor gene, *PTEN. Hum Reprod* 2009; 24: 1036–44.

31 Mithraprabhu S, Loveland KL. Control of KIT signalling in male germ cells: what can we learn from other systems? *Reproduction* 2009; 138: 743–57.

32 Geisinger A, Benavente R. Mutations in genes coding for synaptonemal complex proteins and their impact on human fertility. *Cytogenet Genome Res* 2016; 150: 77–85.

33 Tarsounas M, Morita T, Pearlman RE, Moens PB. RAD51 and DMC1 form mixed complexes associated with mouse meiotic chromosome cores and synaptonemal complexes. *J Cell Biol* 1999; 147: 207–20.

34 Masson JY, West SC. The Rad51 and Dmc1 recombinases: a non-identical twin relationship. *Trends Biochem Sci* 2001; 26: 131–6.

35 Cena A, Kurlandzka A. [Sister chromatid cohesion complex in Eukaryota]. *Postepy Biochem* 2010; 56: 41–54. [Article in Polish].

36 Teletin M, Vernet N, Ghyselinck NB, Mark M. Roles of retinoic acid in germ cell differentiation. *Curr Top Dev Biol* 2017; 125: 191–225.

37 Griswold MD. Spermatogenesis: the commitment to meiosis. *Physiol Rev* 2016; 96: 1–17.

38 Hofmann MC, Narisawa S, Hess RA, Millan JL. Immortalization of germ cells and somatic testicular cells using the SV40 large T antigen. *Exp Cell Res* 1992; 201: 417–35.

39 Hobbs RM, Fagoonee S, Papa A, Webster K, Altruda F, *et al.* Functional antagonism between Sall4 and Plzf defines germline progenitors. *Cell Stem Cell* 2012; 10: 284–98.

40 Sinha N, Puri P, Nairn AC, Vijayaraghavan S. Selective ablation of *Ppp1cc* gene in testicular germ cells causes oligo-teratozoospermia and infertility in mice. *Biol Reprod* 2013; 89: 128.

41 Bao J, Ma HY, Schuster A, Lin YM, Yan W. Incomplete cre-mediated excision leads to phenotypic differences between *Stra8-iCre*; *Mov10l1*^lox/lox and *Stra8-iCre*; *Mov10l1*^lox/Δ mice. *Genesis* 2013; 51: 481–90.

42 Kontaridis MI, Yang W, Bence KK, Cullen D, Wang B, *et al.* Deletion of *Ptpn11* (Shp2) in cardiomyocytes causes dilated cardiomyopathy via effects on the extracellular signal-regulated kinase/mitogen-activated protein kinase and RhoA signaling pathways. *Circulation* 2008; 117: 1423–35.

43 Bard-Chapeau EA, Yuan J, Droin N, Long S, Zhang EE, *et al.* Concerted functions of Gab1 and Shp2 in liver regeneration and hepatoprotection. *Mol Cell Biol* 2006; 26: 4664–74.

44 Zhang SS, Hao E, Yu J, Liu W, Wang J, *et al.* Coordinated regulation by Shp2 tyrosine phosphatase of signaling events controlling insulin biosynthesis in pancreatic beta-cells. *Proc Natl Acad Sci U S A* 2009; 106: 7531–6.

45 Yang W, Klaman LD, Chen B, Araki T, Harada H, *et al.* An Shp2/SFK/Ras/Erk signaling pathway controls trophoblast stem cell survival. *Dev Cell* 2006; 10: 317–27.

46 Reddy RJ, Gajadhar AS, Swenson EJ, Rothenberg DA, Curran TG, *et al.* Early signaling dynamics of the epidermal growth factor receptor. *Proc Natl Acad Sci U S A* 2016; 113: 3114–9.

47 Perrinjaquet M, Vilar M, Ibanez CF. Protein-tyrosine phosphatase SHP2 contributes to GDNF neurotrophic activity through direct binding to phospho-Tyr687 in the RET receptor tyrosine kinase. *J Biol Chem* 2010; 285: 31867–75.

48 Drumond AL, Meistrich ML, Chiarini-Garcia H. Spermatogonial morphology and kinetics during testis development in mice: a high-resolution light microscopy approach. *Reproduction* 2011; 142: 145–55.

49 Bao J, Zhang Y, Schuster AS, Ortogero N, Nilsson EE, *et al.* Conditional inactivation of *Miwi2* reveals that MIWI2 is only essential for prospermatogonial development in mice. *Cell Death Differ* 2014; 21: 783–96.

50 Huszar JM, Jia Y, Reddy JK, Payne CJ. Med1 regulates meiotic progression during spermatogenesis in mice. *Reproduction* 2015; 149: 597–604.

51 Malkov M, Fisher Y, Don J. Developmental schedule of the postnatal rat testis determined by flow cytometry. *Biol Reprod* 1998; 59: 84–92.

52 Sausgruber N, Coissieux MM, Britschgi A, Wyckoff J, Aceto N, *et al.* Tyrosine phosphatase SHP2 increases cell motility in triple-negative breast cancer through the activation of SRC-family kinases. *Oncogene* 2015; 34: 2272–8.

53 Zhang W, Chan RJ, Chen H, Yang Z, He Y, *et al.* Negative regulation of Stat3 by activating *PTPN11* mutants contributes to the pathogenesis of Noonan syndrome and juvenile myelomonocytic leukemia. *J Biol Chem* 2009; 284: 22353–63.

54 Tartaglia M, Niemeyer CM, Fragale A, Song X, Buechner J, *et al.* Somatic mutations in *PTPN11* in juvenile myelomonocytic leukemia, myelodysplastic syndromes and acute myeloid leukemia. *Nat Genet* 2003; 34: 148–50.

55 Sun X, Ren Y, Gunawan S, Teng P, Chen Z, *et al.* Selective inhibition of leukemia-associated SHP2^E69K mutant by the allosteric SHP2 inhibitor SHP099. *Leukemia* 2018; 32: 1246–9.

56 Chen YN, LaMarche MJ, Chan HM, Fekkes P, Garcia-Fortanet J, *et al.* Allosteric inhibition of SHP2 phosphatase inhibits cancers driven by receptor tyrosine kinases. *Nature* 2016; 535: 148–52.

57 Schramm C, Edwards MA, Krenz M. New approaches to prevent LEOPARD syndrome-associated cardiac hypertrophy by specifically targeting Shp2-dependent signaling. *J Biol Chem* 2013; 288: 18335–44.

58 Bowen ME, Boyden ED, Holm IA, Campos-Xavier B, Bonafe L, *et al.* Loss-of-function mutations in *PTPN11* cause metachondromatosis, but not Ollier disease or Maffucci syndrome. *PLoS Genet* 2011; 7: e1002050.

59 Schramm C, Fine DM, Edwards MA, Reeb AN, Krenz M. The *PTPN11* loss-of-function mutation Q510E-Shp2 causes hypertrophic cardiomyopathy by dysregulating mTOR signaling. *Am J Physiol Heart Circ Physiol* 2012; 302: H231–43.

60 Kontaridis MI, Swanson KD, David FS, Barford D, Neel BG. *PTPN11* (Shp2) mutations in LEOPARD syndrome have dominant negative, not activating, effects. *J Biol Chem* 2006; 281: 6785–92.
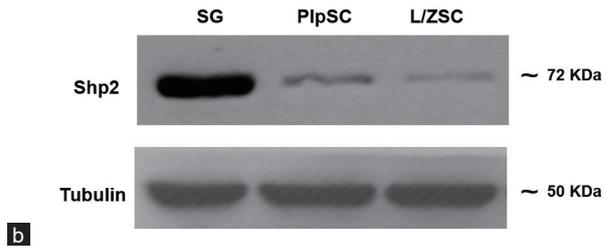
Supplementary Figure 1: Purification of different germ cells from mouse testes. (**a**) Confirmation of the purity of SG, PlpSC, and L/ZSC isolation from control and GCKO mice by cytological classification. Isolated germ cells were immunolabeled with Sycp3, a component of the synaptonemal complex that shows a meiotic substage-specific labeling pattern. Nuclei were counterstained with DAPI. Brown, white, and red yellow arrowheads indicate preleptotene, leptotene, and zygotene spermatocytes, respectively. Scale bar: 50 μm. (**b**) The purity of SG, PlpSCs, and L/ZSCs after isolation from control and GCKO mice was further assessed by RT-PCR analysis of male germ cell-specific marker genes (Plzf and Gfra1 for SG; Rec8 and Prdm9 for PlpSCs; and no specific marker for L/ZSCs). GAPDH was used as a reference control. The data are shown as the mean (±s.d.) of three separate experiments performed in triplicate. Vasa: synaptonemal complex 3; Shp2: promyelocytic leukemia zinc finger; Gfra1: glial cell line derived neurotrophic factor family receptor alpha 1; Rec8: rec8 meiotic recombination protein; Prdm9: PR domain containing 9; DAPI: diamidino-phenyl-indole; SG: spermatogonia; PlpSC: preleptotene spermatocyte; L/ZSC: leptotene/zygotene spermatocyte; Con: control mice; GCKO: germ cell-specific Shp2 knockout mice; s.d.: standard deviation.

Supplementary Figure 2: Shp2 expression pattern during mouse germ cell development. (**a**) Shp2 expression in the seminiferous tubules of testes from adult mice detected by IF staining. Testicular sections were stained for Vasa (red), Shp2 (green), and DAPI (blue). Gray, yellow, white, red, and blue arrowheads indicate Sertoli cells, spermatogonia, spermatocytes, round spermatids, and spermatids, respectively. Scale bar: 50 μm. (**b**) Shp2 protein levels analyzed by Western blot in purified spermatogenic cells (detailed in **Supplementary Figure 1**). Tubulin was used as a loading control. SG; PlpSCs; L/ZSCs. Shp2: Src homology domain tyrosine phosphatase 2; Vasa: DEAD (Asp-Glu-Ala-Asp) box polypeptide 4; DAPI: diamidino-phenyl-indole; SG: spermatogonia; PlpSC: preleptotene spermatocyte; L/ZSCs: leptotene/zygotene spermatocytes; IF: immunofluorescence.

Supplementary Figure 3: The overall status of Shp2 knockout efficiency in GCKO mice. The overall status of Shp2 knockout was assessed by immunostaining for Shp2 (red) and DAPI (blue) in 4- and 8-week-old control and GCKO mice. Yellow arrowheads indicate germ cells with incomplete ablation of Shp2 expression, and white arrowheads indicate Shp2 knockout germ cells. Scale bar: 50 μm. Shp2: Src homology domain tyrosine phosphatase 2; DAPI: diamidino-phenyl-indole; Con: control mice; GCKO: germ cell-specific Shp2 knockout mice; W: weeks.
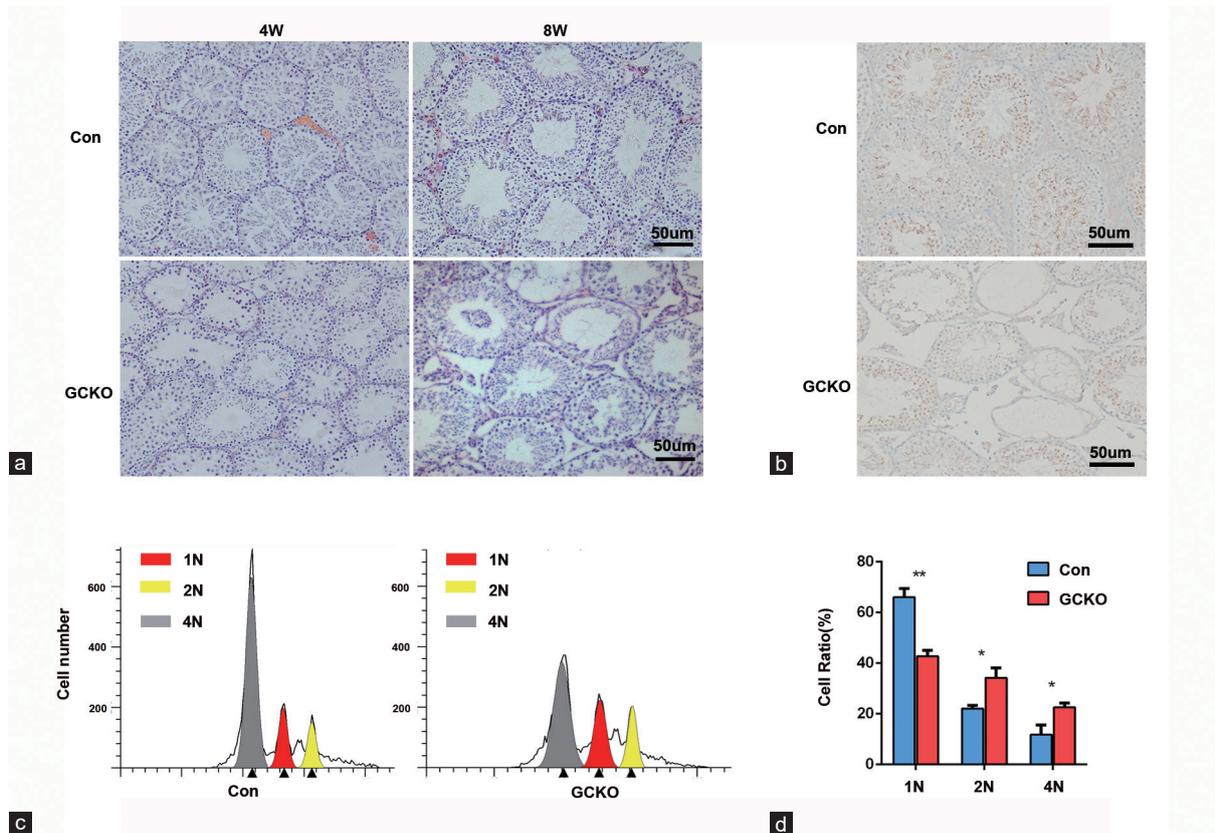
Supplementary Figure 4: Shp2 deletion and spermatogenesis. (**a**) The histological structure of the seminiferous epithelium stained with H and E in control and GCKO mice at 4 and 8 weeks. Scale bar = 50 μm. (**b**) Round spermatids in seminiferous tubules from 8-week-old control mice and GCKO mice shown by immunohistochemical staining for Acvr1 (a round spermatid marker). Scale bar = 50 μm. The experiments were repeated at least three times, and one representative result is presented. (**c**) The overall status of germ cells ratio from 8-week-old control mice and GCKO mice was assessed by flow cytometry after PI staining. Multiple experiments were taken, and representative data are presented. (**d**) Quantification of the number of haploid (1N), diploid (2N), and tetraploid (4N) germ cells as described in (**c**), data are shown as the mean (±s.d.) ($n = 3$, $^{**}P < 0.01$; $^{*}P < 0.05$). The number of haploid, diploid, and tetraploid germ cells was compared between control and GCKO testes. Con: control mice; GCKO: germ cell-specific Shp2 knockout mice; W: weeks; 1N: haploid germ cell; 2N: diploid germ cell; 4N: tetraploid germ cell; H and E: hematoxylin and eosin; s.d.: standard deviation.
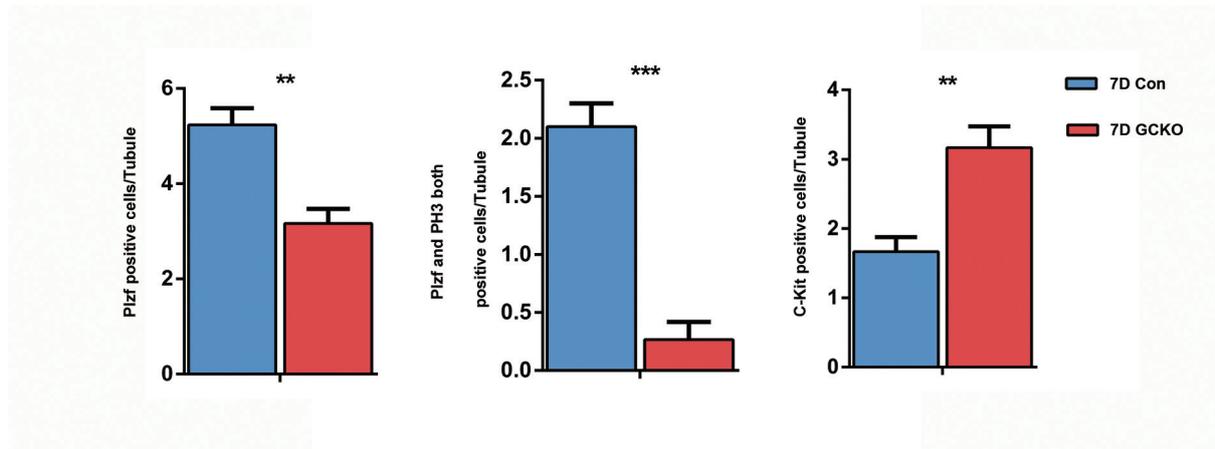
Supplementary Figure 5: Quantification of the number of Plzf+, Plzf/PH3+, and c-Kit+ cells in **Figure 2**. Data are presented as the mean (±s.d.) of at least 5 mice from different litters. $^{*}P < 0.05$; $^{**}P < 0.01$; $^{***}P < 0.001$. The number of Plzf+, Plzf/PH3+, and c-Kit+ were compared between control and GCKO testes. Con: control mice; GCKO: germ cell-specific Shp2 knockout mice; Plzf: promyelocytic leukemia zinc finger; PH3: Phosphorylated histone H3; c-Kit: KIT proto-oncogene and receptor tyrosine kinase; W: weeks; NS: not significant; s.d.: standard deviation.
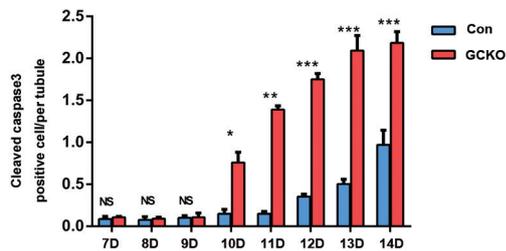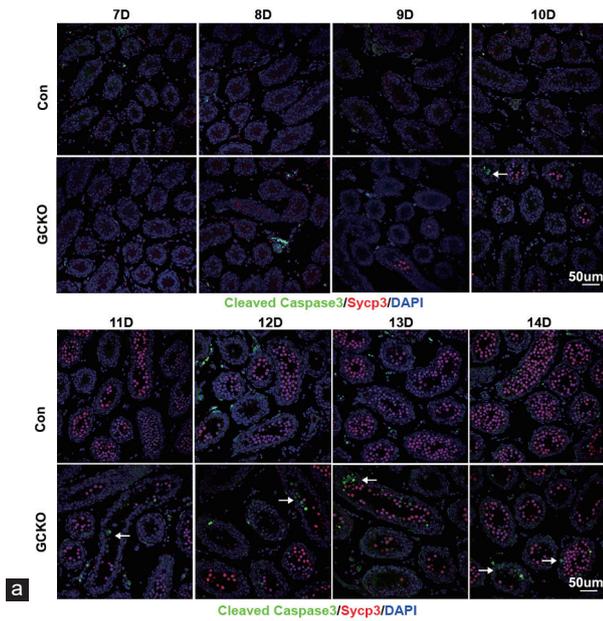
Supplementary Figure 6: The effect of Shp2 deletion on caspase 3 cleavage. (**a**) Cell apoptosis was analyzed by immunostaining for cleaved caspase 3 (green) in the testis tissue from 7-14-day-old control and GCKO mice. Sycp3 (red) is a meiotic spermatocyte marker. Multiple photographs were taken, and representative images are presented. Scale bar: 50 μm. (**b**) Quantification of the number of cleaved caspase 3-positive cells per tubule at the transverse tubule sections of the testes. The cell nucleus was stained with DAPI. The values are expressed as the mean (±s.d.) from at least 5 mice from different litters. Statistical analysis was performed using Student's *t*-test. Asterisks denote statistical significance: *$P < 0.05$; **$P < 0.01$; ***$P < 0.001$. Cleaved caspase 3-positive cells per tubule in the testes sections were compared between control and GCKO testes at same time point. Con: control mice; GCKO: germ cell-specific Shp2 knockout mice; Sycp3: synaptonemal complex 3; DAPI: diamidino-phenyl-indole; D: days; NS: not significant; s.d.: standard deviation.

Supplementary Table 1: Primer sequences for reverse transcription polymerase chain reaction and mouse genotyping

Name of gene	Forward primer sequence (5' to 3')	Reverse primer sequence (5' to 3')	PrimerBank ID
Spo11	GCGTGGCCTCTAGGTTTGAT	CTGATTTTGGTGAATCGCTTCTG	5453472a1
Prdm9	ACCAAAGGCAAGCAATGAAACC	GGACGTGTTCTGAGCCACT	226958681c2
Dmc1	ATGAAGGAGGATCAAGTTGTGC	CATGCTTCTGCAACAGGTCAA	26345652a1
Rad51	AAGTTTTGGTCCACAGCCTATTT	CGGTGCATAAGCAACAGCC	6755276a1
Msh4	CTGCGCGATTACAGCACTG	GTGGCTTCGAGCACTCCAA	13994197a1
Sycp1	TGAGGGGAAGCTCACGGTT	CGAACAGTGTGAAGGGCTTTTG	735904a1
Sycp3	AGCCAGTAACCAGAAAATTGAGC	CCACTGCTGCAACACATTCATA	6755704a1
Syce2	ACCACAGCAAAATCATTCAGGA	GGCAGACTTGTTTAAGCTCCAT	270132238c1
Smc3	AGCAGCGATTGGCTTTGTTG	CCGGTTGTCCGAATTGTCAAAAA	157951634c2
Stag1	GCTGGCAGCGAACTTGAAG	TGTAAGGGGGTAGTCACCACT	26335591a1
Gfra1	TGCGTATCTACTGGAGCATGT	CATCGAGGCAGTTGTTCCCTT	34328183c2
Zbtb16(Plzf)	CTGGGACTTTGTGCGATGTG	CGGTGGAAGAGGATCTCAAACA	142382613c1
Etv5	CGAGTTGTCGTCCTGTAGCC	GGCACAATAGTTGTAGAGGCAC	24528549c3
Bcl6B	GGCTACGTCCGAGAGTTCAC	CTTGTGCGCTCTTAGGGGT	6671616a1
Rec8	TATGTGCTGGTAAGAGTGCAAC	GGATGTCTTCCACAAGGTACTG	326368227c1
Dazl	ATACCTCCGGCTTATACAACTGT	GACTTCTTTTGCGGGCCATTT	188497664c3
Sox3	GCCGACTGGAAACTGCTGA	CGTAGCGGTGCATCTGAGG	6678071a1
c-Kit	GCCACGTCTCAGCCATCTG	GTCGCCAGCTTCAACTATTAACT	10863917a1
Stra8(For mouse genotyping)	TTTGACGTGGCAAGTTTCCTG	TAACACAGCCAAGGCTTTTGA	

Spo11: initiator of meiotic double stranded breaks; Prdm9: PR domain containing 9; Dmc1: DNA meiotic recombinase 1; Rad51: DNA repair recombinase rad51; Msh4: mutS homolog 4; Sycp1: synaptonemal complex protein 1; Sycp3: synaptonemal complex protein 3; Syce2: synaptonemal complex central element protein 2; Smc3: structural maintenance of chromosomes 3; Stag1: stromal antigen 1; Gfra1: glial cell line-derived neurotrophic factor family receptor alpha 1; Zbtb16(Plzf): promyelocytic leukemia zinc finger; Etv5: ets variant 5; Bcl6B: B cell CLL/lymphoma 6, member B; Rec8: rec8 meiotic recombination protein; Dazl: deleted in azoospermia like; Sox3: SRY-box 3; c-Kit: KIT proto-oncogene and receptor tyrosine kinase; Stra8: stimulated by retinoic acid gene 8

Supplementary Table 2: Male fertility evaluation by successive mating with wild type female mice

Genotype (♂)	Number of litters	Total number of pups	Average pups per litter
Shp2$^{f/f}$ (n=8)	77	532	6.91
Shp2$^{f/ko}$ (n=7)	67	461	6.88 (NS)
GCKO (n=8)	68	310	4.56**

Average pups per litter between Shp2$^{f/f}$ and Shp2$^{f/ko}$ male mice are NS. Control (Shp2$^{f/ko}$) and GCKO are significantly different (**$P<0.01$). ♂: male; Shp2: Src homology domain tyrosine phosphatase 2; GCKO: germ cell-specific knockout mice; NS: not significant

Supplementary Table 3: The analysis of genotype of pups in Supplementary Table 2

Father genotype	Pup genotype			
	Stra8-cre null/+ (%)	Stra8-cre F/+ (%)	Null/+ (%)	F/+ (%)
Shp2$^{f/f}$	0	0	0	100
Shp2$^{f/null}$	0	0	47	53
GCKO	15	19	37	29

Shp2: Src homology domain tyrosine phosphatase 2; Stra8: stimulated by retinoic acid gene 8; GCKO: germ cell-specific Shp2 knockout mice